

**DESIGN AND DEVELOPMENT OF A FIXED-
WING VERTICAL TAKE-OFF AND LANDING
UNMANNED AERIAL VEHICLE**

LESTER WONG SENG MAN

**SCHOOL OF AEROSPACE ENGINEERING
UNIVERSITI SAINS MALAYSIA
2018**

**DESIGN AND DEVELOPMENT OF A FIXED-WING VERTICAL TAKE-OFF
AND LANDING UNMANNED AERIAL VEHICLE**

by

LESTER WONG SENG MAN

**Thesis submitted in fulfilment of the requirements for the
Bachelor Degree of Engineering (Honours) (Aerospace Engineering)**

June 2018

ENDORSEMENT

I, Lester Wong Seng Man hereby declare that all corrections and comments made by the supervisor and examiner have been taken consideration and rectified accordingly.

(Signature of Student)

Date:

(Signature of Supervisor)

Name:

Date:

(Signature of Examiner)

Name:

Date:

DECLARATION

This thesis is the result of my own investigation, except where otherwise stated and has not previously been accepted in substance for any degree and is not being concurrently submitted in candidature for any other degree.

(Signature of Student)

Date:

ACKNOWLEDGEMENTS

I, Lester Wong Seng Man have taken efforts in this Final Year Project (FYP), but it will not be possible without the help and support from many individuals. I would like to extend my gratitude to all of them.

I am highly indebted to Dr. Ho Hann Woei (Supervisor) for his guidance and constant advice as well as for providing necessary information on this project and also for his support in completing the project.

I would like to express my gratitude towards the Dr. Ahmad Faizul Hawary, Ir. Dr. Parvathy Rajendran, Mr. Mohd Amir bin Wahab, Mr. Hasfizan bin Hashim, Mr. Abdul Hisham bin Sulaiman, Mr. Mohd Shahar bin Che Had@Mohd Noh, Mr. Mohd Najib bin Mohd Hussian and others for their kind co-operation, attention and time which help me in completion of this project.

Last but not least, my thanks and appreciations also go to my course mates in developing the project and people who have willingly helped us out with their abilities. The skills and knowledge which I gained throughout the whole project, I perceive as very valuable component in my future career development.

DESIGN AND DEVELOPMENT OF A FIXED-WING VERTICAL TAKE-OFF AND LANDING UNMANNED AERIAL VEHICLE

ABSTRACT

The interest in building hybrid Unmanned Aerial Vehicles (UAVs) are increasing intensively due to its capability to perform Vertical Take-Off and Landing (VTOL), in addition to the forward flight mode. With the capability, the hybrid UAVs are highly on demand in various industries such as military, agricultural, and geographic. Unfortunately, hybrid UAVs are facing certain challenges such as the strong crosswind condition during hover mode, complexity in transition flight regime analysis, and the high-cost prototype manufacturing. Taking the challenges into consideration, the fixed-wing VTOL UAV was designed and developed with few focuses during the entire process. The design was optimized to achieve the best flight performance in terms of weight estimation, aerodynamic, propulsion, and stability and control by using Matlab, XFLR5, and Computer Aided Design (CAD) such as SolidWorks. With the allocated time and financial support, a low-cost prototype was developed and fabricated according to the optimized result. Lay-up process was integrated into the prototype fabrication to ensure the high strength structure. Next, testing in actual conditions was needed that led the prototype to flight test. The fixed-wing VTOL UAV was able to take-off vertically with an unstable flight that controlled manually. Therefore, possible next step is to design a controller that allows the fixed-wing VTOL UAV to be controlled and stabilized autonomously in order to achieve the best flight performance.

**REKA BENTUK DAN PENGEMBANGAN PESAWAT UDARA TANPA
PEMANDU YANG BERSAYAP TETAP DENGAN KONFIGURASI
PELEPASAN DAN PENDARAT MENEGAK**

ABSTRAK

Kepentingan dalam membina pesawat udara tanpa pemandu (UAV) hibrid meningkat secara intensif kerana keupayaan untuk melaksanakan operasi konfigurasi pelepasan dan pendarat menegak, selain daripada mod penerbangan ke hadapan. Dengan keupayaan tersebut, UAV hibrid amat diperlukan di pelbagai industri seperti tentera, pertanian, dan geografi. Malangnya, UAV hibrid menghadapi cabaran-cabaran tertentu seperti keadaan angin yang kuat semasa hover, kerumitan analisis rejim penerbangan peralihan, dan pengeluaran prototaip yang kos tinggi. Dengan mengambil kira, pesawat udara tanpa pemandu yang bersayap tetap direka dan dibangunkan dengan sedikit tumpuan sepanjang keseluruhan projek. Reka bentuk dioptimumkan untuk mencapai prestasi penerbangan terbaik dari segi penganggaran berat, aerodinamik, sistem pendorongan, dan kestabilan dan kawalan dengan menggunakan Matlab, XFLR5, dan reka bentuk bantuan komputer seperti SolidWorks. Dengan masa yang diperuntukkan dan sokongan kewangan, prototaip kos rendah dibuat berdasarkan hasil yang dioptimumkan. Proses lay-up telah diintegrasikan ke dalam fabrikasi prototaip untuk memastikan struktur yang mempunyai kekuatan tinggi. Seterusnya, percubaan penerbangan menunjukkan bahawa UAV tersebut yang dikawal secara manual boleh berlepas secara menegak dengan penerbangan yang tidak stabil. Oleh itu, kemungkinan langkah seterusnya adalah untuk mereka alat pengawalan yang membolehkan UAV tersebut dikawal secara autonomi untuk mencapai prestasi penerbangan yang terbaik.

TABLE OF CONTENT

ENDORSEMENT	i
DECLARATION	ii
ACKNOWLEDGEMENTS	iii
ABSTRACT	iv
ABSTRAK	v
LIST OF FIGURES	viii
LIST OF TABLES	x
LIST OF SYMBOLS	xi
CHAPTER 1: INTRODUCTION	1
1.1 General Overview	1
1.2 Problem Statement	2
1.3 Objective	3
1.4 Thesis Layout	4
CHAPTER 2: LITERATURE REVIEW	5
CHAPTER 3: METHODOLOGY	9
3.1 Overview	9
3.2 Design Analysis	10
3.2.1 Computer Aided Design (CAD)	10
3.2.2 Weight Estimation	14
3.2.3 Aerodynamics	14
3.2.4 Propulsion	19
3.2.5 Stability and Control	22
3.2.6 Avionic System	26
3.3 Prototype Manufacturing	30
3.3.1 Wing	30
3.3.2 Components Placement	33
3.3.3 Winglet	34
3.3.4 Motor Frame	37
3.3.5 Motor Mounting	38
3.3.6 Assembly	39
3.4 Flight Test	40
CHAPTER 4: RESULTS AND DISCUSSION	43
4.1 Design Analysis	43
4.1.1 Aerodynamic	43
4.1.2 Winglet	50
4.1.3 Propulsion	50

4.1.4	Stability Analysis	52
4.1.5	Optimized Specification	53
4.2	Prototype Manufacturing	54
4.3	Flight Test	56
CHAPTER 5: CONCLUSIONS AND RECOMMENDATIONS		60
REFERENCES		62
APPENDICES		64
	Appendix A: Aerodynamic Matlab Code	64
	Appendix B: Propulsion Analysis Matlab Code	68
	Appendix C: Simulated propeller's diameter and pitch size	71
	Appendix D: Datasheet of brushless motor RCX07-555	73
	Appendix E: Costing	75

LIST OF FIGURES

Figure 2.1: Existing hybrid UAVs	5
Figure 2.2: Reflex airfoil shape (N, 2015)	6
Figure 3.1: The overall methodology flow chart	9
Figure 3.2: The 4 different views of the fixed-wing VTOL UAV	11
Figure 3.3: The preliminary design of the fixed-wing VTOL UAV	13
Figure 3.4: Graph of moment coefficient against angle of attack (Nelson, 1998)	23
Figure 3.5: Top view wing and aileron (Sadraey, 2012)	24
Figure 3.6: The unbalanced force that is recompensed by the thrust from the side propellers	25
Figure 3.7: Labelling of the distances of side propellers and tractor propeller	26
Figure 3.8: The block diagram of the general architecture of the system	27
Figure 3.9: Printed airfoils are attached to the cardboard	30
Figure 3.10: The flow of fabricating one side of the wing	31
Figure 3.11: The vacuum bag that contain the wing and the mold.	32
Figure 3.12: The flow of the wing fabrication after the resin was cured	33
Figure 3.13: The 2D drawings of the dimensions in mm for the components and structure placement	33
Figure 3.14: The outcome of the components' holes	34
Figure 3.15: The 2D drawing of the winglet design with dimensions in mm	34
Figure 3.16: The flow of the winglets' fabrication	36
Figure 3.17: Improvised winglets	36
Figure 3.18: The motor frame design	37
Figure 3.19: The 2D drawing of the motor mounting with dimensions in mm.	38
Figure 3.20: The motor mounting final product	38

Figure 3.21: Flow of fixed-wing VTOL UAV assembly	40
Figure 3.22: The overall set-up for the flight test	41
Figure 4.1: The full analysis result from XFLR5 for airfoil	43
Figure 4.2: Graph of lift coefficient vs angle of attack for airfoil (Magnified version)	44
Figure 4.3: Graph of lift-to-drag ratio vs angle of attack for airfoil (Magnified version)	45
Figure 4.4: The Moment coefficient vs angle of attack (Magnified version)	46
Figure 4.5: Graph of lift coefficient against angle of attack for wing	47
Figure 4.6: Graph of drag coefficient against angle of attack for wing	48
Figure 4.7: Graph of optimized lift-to-drag ratio against angle of attack for wing	49
Figure 4.8: The selected propellers	51
Figure 4.9: Graph of moment coefficient vs angle of attack for wing-body where left image is XFLR5 analysis and right image is theoretical analysis (Nelson, 1998)	52
Figure 4.10: 4 different views of the fixed-wing VTOL UAV	54
Figure 4.11: Isometric view of the fixed-wing VTOL UAV with every part labelled	55
Figure 4.12: The cables connection between motor and ESC (Sam, 2015)	58

LIST OF TABLES

Table 3.1: The basic initial parameters of the fixed-wing VTOL UAV	14
Table 3.2: Summary of the algorithm flow for aerodynamic analysis	17
Table 3.3: Summary of the algorithm for propulsion analysis	20
Table 3.4: Principle axis and motion for an aircraft (Nelson, 1998)	22
Table 3.5: Typical guidance for the ailerons sizing	23
Table 3.6: Electronic components used in this design	27
Table 3.7: Values for woven glass fiber's mass and resin mixture for wing structure	32
Table 3.8: The mass values for woven glass fibers and resin mixture	35
Table 4.1: The optimized result of the wing configuration	49
Table 4.2: Parameters of winglet	50
Table 4.3: Result of the fixed-wing VTOL UAV propulsion system	50
Table 4.4: The optimized aileron parameters	52
Table 4.5: The optimized sizing for the fixed-wing VTOL UAV	53
Table 4.6: The specification for new ESC	57

LIST OF SYMBOLS

a_o	:	Airfoil lift slope
ac	:	Aerodynamic centre [m]
AR_{wing}	:	Aspect ratio of wing
AR_V	:	Aspect ratio of stabilizer
b_a	:	Aileron span [m]
b_{ai}	:	Location of inner edge of the aileron along the wing span [m]
b_{wing}	:	Wing span [m]
b_V	:	Stabilizer span [m]
C_a	:	Aileron chord [m]
C_d	:	Induced drag coefficient
C_{D_wing}	:	Drag coefficient of wing
cg	:	Centre of gravity [m]
C_l	:	Lift coefficient of airfoil
$C_{l_{max}}$:	Maximum lift coefficient of airfoil
$C_{L_{max_wing}}$:	Maximum lift coefficient of wing
C_{L_wing}	:	Lift coefficient of the wing
$C_{m_{ac}}$:	Moment coefficient of aerodynamic centre
$C_{m\alpha}$:	Moment slope coefficient
$C_{m0_{cg}}$:	Zero angle of attack moment coefficient about centre of gravity
C_{m_o}	:	Zero angle of attack of moment coefficient
C_{r_wing}	:	Root chord length [m]

C_{t_wing}	:	Tip chord length [m]
c_{wing}	:	mean aerodynamic chord of wing [m]
$C_{V_{root}}$:	Root chord length of the stabilizer [m]
$C_{V_{tip}}$:	Tip chord length of the stabilizer [m]
c_V	:	Mean aerodynamic chord length of stabilizer [m]
d_{side}	:	Distance of the side propeller [m]
$d_{tractor}$:	Distance of the tractor propeller to the centre of gravity [m]
$Diam$:	Diameter of propeller [m]
D_{wing}	:	Drag of wing [N]
e	:	Oswald efficiency number
eff_{motor}	:	electric motor efficiency [%]
g	:	Universal constant of gravitational [$6.669 \times 10^{-11} \text{ m}^3\text{kg}^{-1}\text{s}^{-2}$]
I_{motor}	:	Current of motor [A]
L_{wing}	:	Lift of wing [N]
$Pitch$:	Pitch size of propeller [m]
$P_{motor-in}$:	Power into the motor from the battery [W]
$P_{motor-out}$:	Power out of the motor from the battery [W]
$P_{prop-in}$:	Power from the electric motor to the propeller [W]
$P_{prop-req}$:	Power required from the propeller [W]
RN	:	Reynolds number
RPM	:	Propeller revolution per minute [rpm]
S_a	:	Aileron planform area [m^2]
S_{wing}	:	Area of wing [m^2]
T_{side}	:	Thrust produced by the side propeller [N]

$Thrust_{prop}$:	Propeller thrust [N]
V	:	Airspeed [m/s ²]
V_{motor}	:	Voltage of motor [V]
$V_{prop-pitch}$:	Velocity of the propeller pitch [m/s ²]
$V_{prop-tip-static}$:	Propeller tip static velocity [m/s ²]
V_{stall}	:	Stall velocity [m/s ²]
$W_{propulsion}$:	Weight of overall propulsion [kg]
$W_{payload}$:	Weight of overall payload [kg]
$W_{structure}$:	Weight of overall structure [kg]
W_{TOmax}	:	Maximum take-off weight [kg or N]
λ_{wing}	:	Taper ratio of wing
λ_V	:	Taper ratio of stabilizer
Λ_{le_wing}	:	Leading edge swept angle of wing [°]
Λ_{le_V}	:	Leading edge swept angle of stabilizer [°]
α	:	Angle of attack [°]
ρ	:	Density [1.225 kg/m ³]
μ	:	Viscosity [1.82 x 10 ⁻⁵ Pa.s]
δ_{Amax}	:	Maximum aileron deflection [°]
$\tau_{tractor}$:	Torque produced by the tractor propeller [N.m]
τ_{side}	:	Torque produced by the side propeller [N.m]

CHAPTER 1

INTRODUCTION

1.1 General Overview

Recently, aerospace community has been showing a great interest in Unmanned Aerial Vehicle (UAV) because of the ability to carry out certain missions involving surveillance, wildlife tracking and disaster support (Aktas et al., 2016). UAVs can be divided into two types: fixed-wing UAVs and rotary UAVs that come with its own advantages and disadvantages. The lift generation for both types are different where fixed-wing UAVs generate lift by using its wing and rotary UAVs generate lift by using the thrust from the propellers. Fixed-wing UAVs with efficient aerodynamics are able to fly for a long period of time with a simple design (Cetinsoy et al., 2012) but it requires a runway or launcher, and recovery equipment for take-off and landing. The long flight period enables fixed wing UAVs to accomplish larger survey area per given flight. In contrast, rotary UAVs have the advantage of no infrastructural supports are required such as launcher or runway (Pranay Sinha, 2012). This allow the rotary UAVs to conduct VTOL and stationary operations as fixed wing UAVs require a constant forward motion to generate lift. On the other hand, rotary UAVs are flying at low flight speeds and are unable to perform a long duration mission (Cetinsoy et al., 2012).

In order to acquire the best UAVs configuration, hybrid UAVs are introduced with the combination of both fixed-wing and rotary wing configuration. The hybrid UAVs can be divided into two types: convertiplane and tail-sitter (Donlan, 1944). Convertiplane consists of tilt-rotor (Pranay Sinha, 2012), tilt-wing (Cetinsoy, 2015), rotor-wing (Donlan, 1944) and dual system (Yilmaz et al., 2013). The hybrid configuration is

favourable because it does not require any runway or complex launching mechanism and recovery for take-off and landing, in addition, long duration flight is possible. These advantages tell that hybrid UAVs are useful in a huge range of industrial environment applications such as agriculture, surveillance and payload delivery. Hybrid UAVs have the ability to maneuver Vertical Take-Off and Landing (VTOL) along with high cruise performance (Muraoka et al., 2009). Their hovering and maneuvering capabilities provide exceptional efficiency in terms of observation, monitoring and other missions that require access to dangerous locations. With the efficiencies, the hybrid UAVs portrayed many potential utilization in many areas such as aerial cargo, forest patrolling, pipeline and power line control, and aerial refereeing of sport events (Cetinsoy, 2015). Unfortunately, fixed-wing VTOL UAVs are facing the strong crosswind conditions during hover flight (Moschetta, 2014), the complexity transition flight regime (Aktas et al., 2016) analysis, and the high-cost UAV prototype manufacturing.

1.2 Problem Statement

Recently, there are many VTOL UAVs available in the market but most of them were produced by using high-end technology method such as high precision CNC. The products from the high-end technology are good and efficient. Besides that, previous researchers found that certain fixed-wing VTOL UAVs are facing the strong crosswind condition during hover flight (Moschetta, 2014) and the complexity of the transition flight regime analysis. Furthermore, the range of applications and the design is part of an effort to explore the possibilities of the advantages and disadvantages. The inspiration of developing the fixed-wing VTOL UAV was due to the demand in various applications that could improve the aerospace industry. Thus, a new fixed-wing VTOL UAV design will be developed and analysed in terms of weight estimation, aerodynamic, propulsion,

and stability and control that will help to improve the flight performance. The new fixed-wing VTOL UAV design will be based on the limitations of time, cost and facilities available.

Theoretical analysis itself is not enough to support the workability of the fixed-wing VTOL UAV design. The analysis will remain as a doubt to the actual performance of the design. Thus, it is necessary to manufacture the prototype to test the practicability of the design. With the limitations mentioned beforehand, a low-cost prototype will be developed and fabricated. As the process continued, the design is allowed to change accordingly if there is any unsuccessful ideas or prototype. Lastly, the workability and performance of the prototype will solely depend on the result from the flight test.

1.3 Objective

1. To optimize the fixed-wing VTOL UAV design by analysis to achieve the following performances.
 - Maximum take-off weight: $1.2 \text{ kg} \pm 0.2 \text{ kg}$
 - Optimal aerodynamic performance
 - Maneuverability: Take-off vertically to hover and hover to land vertically.
2. To manufacture one prototype according to the optimized fixed-wing VTOL UAV.
3. To carry out flight test on the prototype.

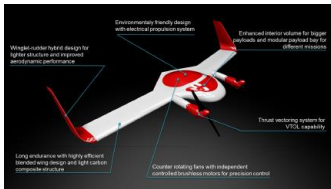
1.4 Thesis Layout

This thesis consists of 5 chapters, introduction, literature review, methodology, results and discussion, and conclusions and recommendation. In chapter 1 which is the introduction that describes on the general overview of this project followed by problem statements and objectives. Chapter 2 describes the study of existing projects from the previous researches regarding fixed-wing VTOL UAVs. Chapter 3 tells the methods used in designing and developing the fixed-wing VTOL UAV that includes the optimization analysis on the performance characteristics, prototype manufacturing and flight test. Chapter 4 shows the analysis optimization result of the fixed-wing VTOL UAV, followed by the prototype outcome and lastly, the flight test result and discussion. Finally, yet importantly, chapter 5 that concludes the thesis with future suggestion in improving the current work.

CHAPTER 2

LITERATURE REVIEW

Nowadays, many fixed-wing VTOL UAVs are built due to their capability in performing VTOL and better cruising performance with transition regime. Few existing VTOL UAVs design are being studied which can be seen from Figure 2.1a. to Figure 2.1i. The survey will help in obtaining general and beginning concept in achieving the performances mentioned in Section 1.3.



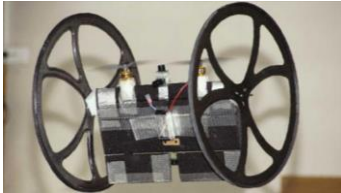
a. TURAC
(Aktas et al., 2016)



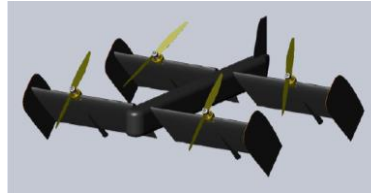
b. DelftaCopter
(De Wagter et al., 2016)



c. Cyclone
(Bronz et al., June 2017)



d. MAVion
(Moschetta, 2014)



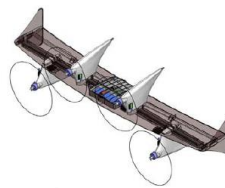
e. SUAVI
(Cetinsoy et al., 2012)



f. Tail-Sitter UAV
(Matsumoto et al., 2010)



g. ITU Tail Sitter UAV
(Aksugur and Inalhan, 2010)



h. QuadShot
(Sinha et al., 2012)



i. Monoplane MAV
'Kiool'
(Moschetta, 2014)

Figure 2.1: Existing hybrid UAVs

Every existing hybrid UAV design produces different performance characteristics but have the similar maneuvers capability which are hovering, transition, and vertically take-off and landing. From the research, tailless concept has better aerodynamic performance such as decreasing in drag that helps to increase the overall lift-to-drag ratio (Karakas et al., 2013), decreasing the nose down movement (Aktas et al., 2016) and avoid the cross wind during VTOL operation (Saengphet and Thumthae, 2016). On the other hand, tailless concept do have the disadvantages in terms of stability and control characteristic that are affected by the location of centre gravity (Karakas et al., 2013). There is a common airfoil used in the tailless concept UAV which is the reflex airfoil shape as shown in Figure 2.2 where there is a slight up curve at the trailing edge (Aktas et al., 2016, Donlan, 1944, Karakas et al., 2013, Sadraey, 2012a, Saengphet and Thumthae, 2016, V.Hogge, 2008). It is used to balance the moment produced from generating lift. Furthermore, it is generated into special wing profile called reflex profile (Karakas et al., 2013, Aktas et al., 2016). The Quadshot uses the symmetrical airfoil so that the inverted operation (Pranay Sinha, 2012) can be achieved without affecting the aerodynamic performance.



Figure 2.2: Reflex airfoil shape (N, 2015)

DelftaCopter and SUAVI are designed with winglet because it provides higher aerodynamic performance (Moschetta, 2014) such as reducing the drag generated from the wingtip vortices. TURAC is designed with winglet-rudder hybrid design which benefits in providing lateral stability (Aktas et al., 2016).

Apart from that, tilting mechanism including rotors or wings which can be called as convertiplane (Saengphet and Thumthae, 2016) that provides the ability to perform

VTOL operations together with transition flight more efficient. Regrettably, the tilting mechanism is more complex and leads a higher power consumption. The tilt-rotors are usually mounted on rotating shaft where the rotors will tilt according to the desired direction of flight path. TURAC (Figure 2.1a) has both fixed and tilt rotors because the fixed wing will give extra lift for take-off, landing and hovering (Aktas et al., 2016). Tilt-wing applies the same concept as tilt rotor where SUAVI has quad tilt wings as shown in Figure 2.1e that has the benefits in payload carrying task and maintenance costs (Muraoka et al., 2009). Generally, UAVs with high cruise performance are in demand where it can be achieved by having tilt wing configuration because it has higher disc loading and smaller diameter propellers than tilt rotor UAVs. Unfortunately, tilt wing creates higher downwash and noise (Muraoka et al., 2009). On the other hand, tail sitter (Figure 2.1f) is another configuration that has the same capability as convertiplane but instead of tilting the rotors or wings, tail sitter UAV tilts the whole UAV using differential thrust (Saengphet and Thumthae, 2016) or control surfaces to fly at the desired direction.

Besides, wing configuration affects greatly on the performance of an aircraft. A bi-plane wing configuration as shown in Figure 2.1b helps in reducing the perturbations of take-off and landing in windy condition because a single wing (Figure 2.1c, 2.1d, 2.1f, 2.1g, 2.1h) has more surface area that is exposed to the wind in VTOL operations (De Wagter et al., 2016). Moreover, a wide range of angle of attack is required to perform the transition from hover to forward flight and back (De Wagter et al., 2016) where bi-plane wing has the capability to do so compared to single wing. Moreover, bi-plane has the advantage in generating higher lift, hence, the payload capacity objective can be achieved. Note that TURAC has single wing configuration but less surface area (Aktas et al., 2016) is exposed to the wind during VTOL mode due to the position of the wing that makes

TURAC a useful design for hovering and forward flight mission as it managed to have high endurance time of 85 minutes (Aktas et al., 2016). An exceptional design from Monoplane MAV 'Kiool' with a V shape stabilizer (Moschetta, 2014) attached to the bottom of the fixed wing. This V shape stabilizer act as a tail to control the pitching and rolling, additionally, the lateral stability without affecting the aerodynamic performance (Moschetta, 2014).

UAV that has low manufacturing cost, impact resistant, portable and lightweight are the concerned to all the designers. Quadshot uses injection molding and Computer Numerical Control (CNC) methods in fabricating the airframe structure and unidirectional-extruded carbon fibre tube is used over woven carbon fibre for the main spar due to low cost, strength and the rigidity (Pranay Sinha, 2012). Besides, TURAC is known with the low-cost prototyping method that starts with a process of foam body production in a CNC counter (Aktas et al., 2016) where 5 different versions were fabricated that serve different missions. In addition, Cyclone uses the same method as TURAC which is CNC (Bronz et al., June 2017) method with aluminium molds. In common, CNC method is used for the fabrication in airframe structure because of its reliability, precision and high-quality outcome with low-cost manufacturing process.

With all the reasoning to every design configuration, a clear view on the design goal for this project will be obtained that will help in estimating the design values of the fixed-wing VTOL UAV.

CHAPTER 3

METHODOLOGY

3.1 Overview

The overall design methodology flow chart is shown in Figure 3.1.

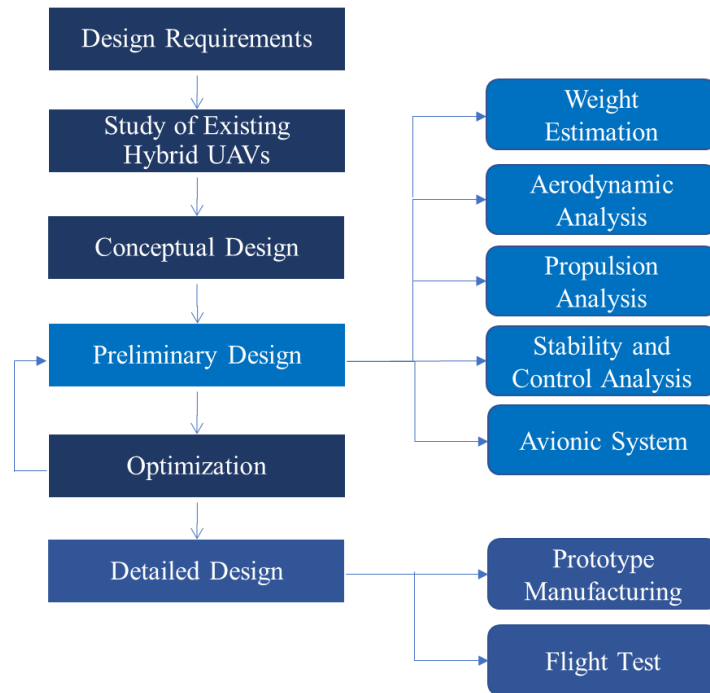


Figure 3.1: The overall methodology flow chart

The methodology of this project starts with the design requirements which fulfill the needs from customers. Next, study on the existing hybrid UAVs was carried out and discussed in Chapter 2. This study is the starting point for the designers to develop a concept leading to the conceptual design on which type of configuration in contributing to the best flight performance.

A preliminary design was completed with the parameters needed to proceed with the weight estimation, aerodynamic, propulsion, stability and control, and avionic system analysis. Optimization analysis was finalized to obtain the best design for a fixed-wing VTOL UAV. Matlab, SolidWorks and XFLR5 were the tools used to analyze the design.

Finally, the detailed design is where the prototype manufacturing and flight test were executed. The flight test was executed to discover the workability of the fabricated prototype.

3.2 Design Analysis

3.2.1 Computer Aided Design (CAD)

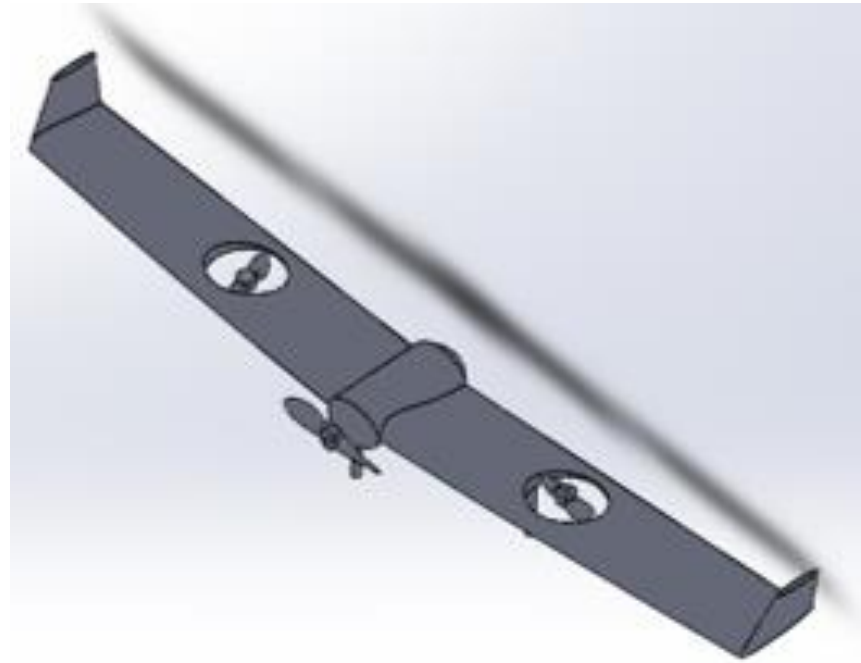
A software called SolidWorks was used to draw the technical drawing includes the 2D and 3D drawings of the fixed-wing VTOL UAV design for this project. The conceptual design was drawn with the ideas obtained from the study of existing UAVs. Next, the preliminary design was drawn with the initial basic parameters.

3.2.1.1 Conceptual Design

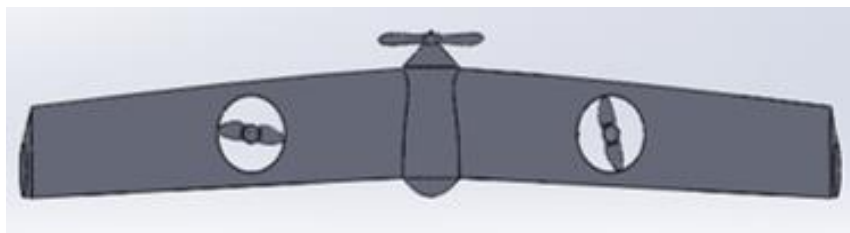
The fixed-wing VTOL UAV is built with a tailless configuration hybrid UAV with blended wing-body design. The conceptual design of the UAV is as shown in Figure 3.2. The UAV is designed with VTOL functionality and 3 propellers are used in this design with different positions. Two propellers are situated on the wing itself which will be used for the vertical take-off operation. Meanwhile, the tractor propeller positioned at the leading edge of the wing will be used for the forward flight operation. The position of the two propellers on the wing will increase the efficiency of the propulsion system due to the ducting effect. The ‘ducting effect’ affects the propeller thrust coefficient where ducted propeller requires less power consumption (Yilmaz et al., 2013) compared to open propeller. The ducted propeller decreases the tip vortex created from the blade of the propeller.



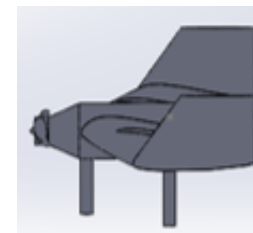
a. Front View



b. Isometric View



c. Top View



d. Side View

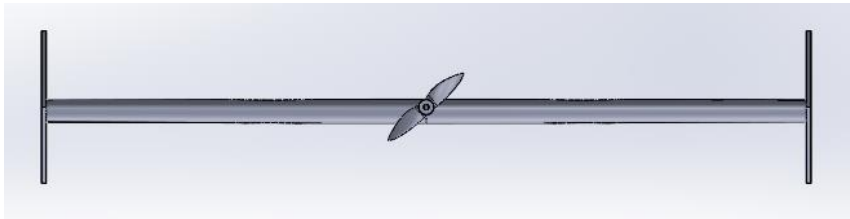
Figure 3.2: The 4 different views of the fixed-wing VTOL UAV

Winglets are added into the design to improve on the aerodynamic performance as winglets help to reduce the wingtip vortices during forward flight. In addition, the winglets will act as rudder that helps in the directional stability and control (Donlan, 1944). The UAV is designed with 3 landing stands that can protect the UAV from any damages when it lands.

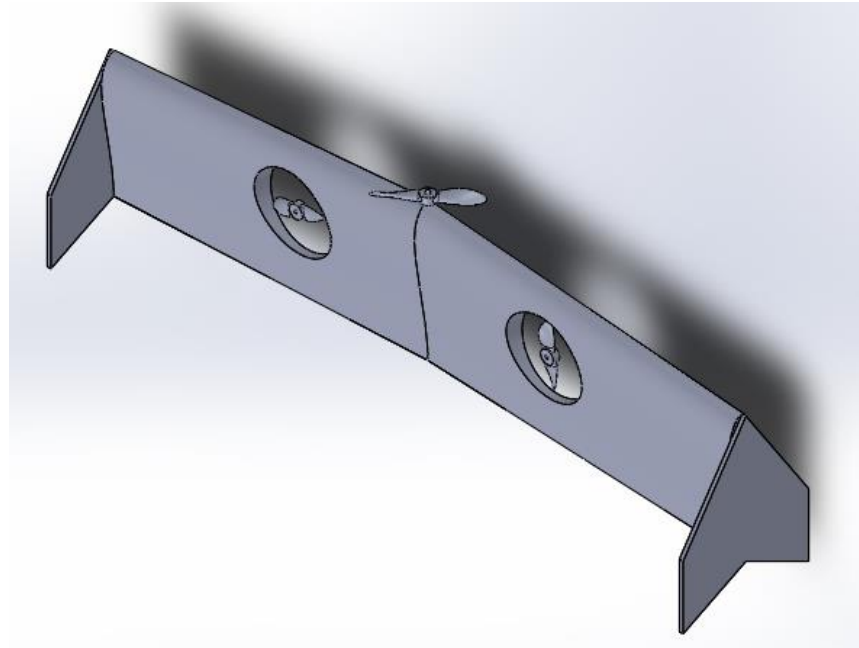
Single wing configuration is chosen for the fixed-wing VTOL UAV design with a small swept angle. Since the UAV is based on a tailless concept, the static stability is the crucial factor. Hence, a proper airfoil with moment coefficient of aerodynamic centre more than 0 ($C_{mac} > 0$) (Karakas et al., 2013) is required. A small swept angle is chosen instead of a large swept angle because of the stability where less twist is required. As a result, less twist will help to ease the prototype fabrication and higher wing structure strength can be obtained.

3.2.1.2 Preliminary Design

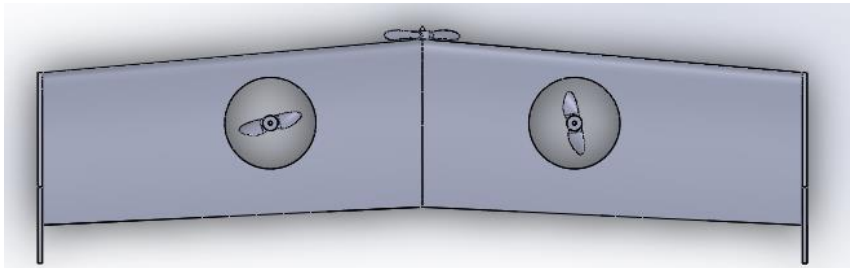
The fixed-wing VTOL UAV design remained the same as discussed earlier but with minor changes. The tractor propeller is used to perform vertical take-off mode where the 2 propellers situated on the wing are used to counter the torque (CNATRA, 2013) produce by the tractor propeller and act as control surfaces during the flight. In addition, the winglets will become the landing stands instead of the 3 landing stands shown in Figure 3.2. Figure 3.3 shows the overall preliminary fixed-wing VTOL UAV design with 4 different views.



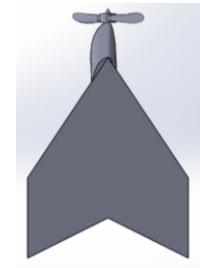
a. Top View



b. Isometric View



c. Front View



d. Side View

Figure 3.3: The preliminary design of the fixed-wing VTOL UAV

The basic initial parameters are listed in Table 3.1. The basic initial parameters were used as a guidance for the following analysis. The parameters will be reassessed according to the analysis optimization.

Table 3.1: The basic initial parameters of the fixed-wing VTOL UAV

No.	Parameter	Dimension
1	Wing span, b_{wing}	1.0 m
2	Root chord length, C_{r_wing}	0.22 m
3	Tip chord length, C_{t_wing}	0.20 m
4	Taper ratio, λ_{wing}	0.91 m
5	Leading edge swept angle, Λ_{le_wing}	5°

3.2.2 Weight Estimation

The initial overall weight of the UAV is calculated using Equation (1) where the weight of the propulsion, payload and structure were obtained from the preliminary selection of the components. The overall weight will be revised after the optimization. As for this project, the weight of the UAV was estimated around $1.2 \text{ kg} \pm 0.2 \text{ kg}$. Kept in mind that the Maximum Take Off Weight (MTOW) of the fixed-wing VTOL UAV must be kept as low as possible to enhance the performance.

$$W_{TO_{max}} = W_{propulsion} + W_{payload} + W_{structure} \quad (1)$$

3.2.3 Aerodynamics

The aerodynamic performance of a fixed-wing VTOL UAV is determined by the total lift and drag. Matlab was used to analyse the aerodynamic performance by referring to the entire Matlab code attached in Appendix A (Ming et al., 2017). Theoretically, the design has to achieve high lift and low drag for the UAV to attain optimal aerodynamic

performance. The lift-to-drag ratio measures the aerodynamic efficiency of an UAV. In order to obtain the high lift-to-drag ratio, the sequence will start from determining the configuration of the airfoil to the wing. The empennage analysis is not incorporated due to the tailless concept chosen.

3.2.3.1 Airfoil

XFLR5 analysis tool is used to analyse the aerodynamic characteristic of an airfoil. XFLR5 is used in a large-scale due to its user-friendly interface of performing the tasks to simulate diverse types of airfoil with different range of Reynold's number and angle of attack. XFLR5 can generate the lift, drag and moment coefficient that will be used in analysis. XFLR5 uses 3 different methods in computing the parameters: Lifting Line method, derived from Prandtl's wing theory; Vortex Lattice method; and 3D panel method. These 3 methods have its own analysing limitations (Matthieu et al., 2009).

There are 8 types of reflexed airfoil being studied in this project, namely, E186, HS 522, MH 60, MH 78, MH 82, MH 92, S 5020 and Sipkill 1,7/10B. These airfoils are studied in terms of C_{mac} , C_{lmax} and lift-to-drag ratio. As mentioned, these airfoils are reflexed airfoils that benefit the tailless UAV configuration in terms of aerodynamics, and stability and control.

Airfoil lift slope, a_o can be formulated by using Equation (2) (John D. Anderson, 1999).

$$a_o = \frac{dC_l}{d\alpha} \quad (2)$$

Note that the range of the angle of attack, α is from -20° to 20° with the Reynolds number of 123,000.

3.2.3.2 Wing

In aircraft design, aspect ratio of a wing is one of the parameter that determine the aerodynamic efficiency because increasing aspect ratio will increase the lift-to-drag ratio. Aspect ratio of a wing is the ratio of square wing span (b_{wing}^2) to its wing area (S_{wing}) which can be written as shown in Equation (3) (John D. Anderson, 1999).

$$AR_{wing} = \frac{b_{wing}^2}{S_{wing}} \quad (3)$$

Reynolds number is an important parameter in determining the type of flow we can expect which is either laminar flow or turbulent flow. Since this is a project that involve small UAV, a low Reynolds number is considered. Reynolds number (RN) depends on the density (ρ), airspeed (V), mean aerodynamic chord (c_{wing}) and viscosity (μ) (John D. Anderson, 1999).

$$RN = \frac{\rho V c_{wing}}{\mu} \quad (4)$$

In determining the lift coefficient of the wing, Equation (5) can be applied (John D. Anderson, 1999).

$$C_{L_wing} = \frac{L_{wing}}{\frac{1}{2} \rho V^2 S_{wing}} \quad (5)$$

Note that two theories were considered in determining the lift coefficient due to the different aspect ratio. If the aspect ratio is more than 4, lifting line theory (John D. Anderson, 1999) is applied whereas aspect ratio less than 4, lifting surface theory (John D. Anderson, 1999) is applied.

In obtaining the drag coefficient instead, Equation (6) can be applied (John D. Anderson, 1999). Only the drag from the wing is considered.

$$C_{D_wing} = \frac{D_{wing}}{\frac{1}{2}\rho V^2 S_{wing}} \quad (6)$$

Besides that, the lift and drag can also be calculated by using Equations (7) and (8) respectively (John D. Anderson, 1999). It is known that during the level flight, the lift of the UAV is equal to the maximum take-off weight (W_{TOmax}) of the UAV. Lastly, the ratio of Equation (7) to (8) gives the value of lift-to-drag ratio. In addition, the stall velocity is the crucial parameter to ensure the speed of the UAV does not fall below the stall velocity. The stall velocity can be obtained by using Equation (9).

$$L_{wing} = W_{TOmax} = \frac{1}{2}\rho V^2 S_{wing} C_{L_wing} \quad (7)$$

$$D_{wing} = \frac{1}{2}\rho V^2 S_{wing} C_{D_wing} \quad (8)$$

$$V_{stall} = \sqrt{\frac{W_{TOmax}}{(\frac{1}{2})\rho C_{Lmax_wing} S_{wing}}} \quad (9)$$

Table 3.2 shows the summary of the algorithm flow for aerodynamic analysis, while the entire Matlab code can be obtained from Appendix A.

Table 3.2: Summary of the algorithm flow for aerodynamic analysis

Algorithm for aerodynamic analysis

For i = 1:11 % 11 types of aspect ratio

Input: The range of tip chord and root chord length

Algorithm Body:

1. Compute the aspect ratio based on Equation (3)
 2. **If** aspect ratio is in the interest range
-

-
3. Compute the induced drag factor value
 4. **End**
 5. Record the Oswald efficiency factor that fulfill the condition
 6. Compute the Reynold number based on Equation (4)
 7. **If** Reynold number is in the interest range
 8. Record the angle of attack, lift coefficient and drag coefficient of airfoil that fulfill the condition
 9. **End**
 10. **If** Aspect ratio is in the interest range
 11. Compute the lift coefficient based on Equation (5) that fulfill the condition
 12. Compute the drag coefficient based on Equation (6) that fulfill the condition
 13. Compute the lift to drag ratio that fulfill the condition
 14. **End**
 15. Plot the graphs
 16. **End**

Output:

1. Find the optimized parameters

$[M,I] = \max(L_D_w(:));$

$[I_row, I_col] = \text{ind2sub}(\text{size}(L_D_w), I);$

2. Plot the optimized graphs
-

3.2.4 Propulsion

Electric propulsion system sizing is a critical parameter to be considered in designing the UAV. Matlab is used as the tool to analyse the propulsion system. The power-to-weight ratio and power-to-thrust ratio are essential in determining the performance of the UAV. Both the parameters can be estimated using Equations (10) and (11) respectively. As suggested by Parvathy Rajendran and Howard Smith (Rajendran and Smith, 2018), the electric motor efficiency, power from the electric motor to the propeller and the power required from the propeller can be estimated from the Equations (12), (13) and (14) respectively.

$$\frac{P}{W} = \frac{P_{motor-in}}{gW_{TO_{max}}} \quad (10)$$

$$\frac{P}{T} = \frac{P_{motor-in}}{gThrust_{prop}} \quad (11)$$

$$eff_{motor} = \frac{P_{motor-out}}{P_{motor-in}} \times 100 \quad (12)$$

$$P_{prop-in} = eff_{motor} V_{motor} I_{motor} \quad (13)$$

$$P_{prop-req} = \frac{0.5\rho}{g} \left(\frac{RPM}{60}\right)^3 (0.0254Diam)^4 (0.0254Pitch) \quad (14)$$

Where $P_{motor-out}$ is the power out of the motor, $P_{motor-in}$ is the power into the motor from the battery, V_{motor} is the motor voltage, I_{motor} is the motor current, RPM is the propeller revolution per minute, $Diam$ is the diameter of the propeller, and $Pitch$ is the pitch size.

Ideally, the value for pitching velocity of the propeller should be within the 2.5 to 3 times the aircraft stall speed (Rajendran and Smith, 2018). In order for the UAV to

have climbing and accelerating capabilities, the estimated propeller thrust must be more than 25% of the maximum take-off weight of the UAV (Rajendran and Smith, 2018).

$$V_{prop-pitch} = \frac{RPM}{60} (0.0254Pitch) \quad (15)$$

$$Thrust_{prop} = \frac{P_{prop-req}}{gV_{prop-pitch}} \quad (16)$$

Next, a list of simulated propeller's diameter and pitch size combination is produced and presented in Appendix C. From the list, the optimized propeller size (diameter and pitch) was selected based on the least propeller tip static velocity (Rajendran and Smith, 2018). Equation (17) shows the formula to estimate the propeller tip static velocity.

$$V_{prop-tip-static} = \pi \frac{RPM}{60} (0.0254Diam) \quad (17)$$

Next, Table 3.3 shows the summary of the algorithm for propulsion analysis, meanwhile the entire code can be obtained from Appendix B (Ming et al., 2017).

Table 3.3: Summary of the algorithm for propulsion analysis

Algorithm for propulsion analysis

Input: Parameters for MTOW, required thrust, battery, ESC, motor, range of propeller size

Algorithm Body:

1. **For** i = 1: length of motor current efficiency
 2. Compute motor efficiency based on Equation (11)
 3. **If** motor power input (i) is smaller or equal to power available
-

-
4. Compute the power propeller input based on Equation (13)
 5. Compute the power propeller output based on Equation (14)
 6. Compute the propeller pitch speed based on Equation (15)
 7. Compute the propeller thrust based on Equation (16)
 8. **If** propeller thrust > MTOW or propeller > drag
 9. Compute propeller tip static speed based on Equation (17)
 10. Compute power to weight ratio and power to thrust ratio
 11. **Else**
 12. **Continue**
 13. **End**
 14. **Else**
 15. **Break**
 16. **End**
 17. **End**

Output:

1. Display the parameters of simulated propeller's diameter and pitch size combination using **xlswrite** command
 2. Choose optimum set based on minimum propeller tip speed
 3. $[M,I] = \min(\text{propeller tip speed}(:));$
 4. $[\text{row}, \text{col}] = \text{ind2sub}(\text{size}(\text{propeller tip speed}), I);$
 5. Record and display the parameters that fulfill the conditions
-

3.2.5 Stability and Control

Flight stability and control is crucial to ensure the design of the UAV is stable and ready to fly. The static stability is the initial stability stage of the UAV design to ensure the position and sizing of the wing, fuselage and empennage are within the range to achieve the stability. The static stability includes longitudinal stability, lateral stability, and directional stability. Table 3.4 shows the principle axis and motion of the stability.

Table 3.4: Principle axis and motion for an aircraft (Nelson, 1998).

No.	Primary Control Surface	Aircraft Movement	Axes of rotation	Type of stability
1	Aileron	Roll	Longitudinal	Lateral
2	Elevator / Stabilizer	Pitch	Lateral	Longitudinal
3	Rudder	Yaw	Vertical	Directional

For the current case, the design of the fixed-wing VTOL UAV is a tailless concept which means that the stability is greatly affected. The lateral stability is compensated by the aileron and the 2 propellers situated on the wing. The longitudinal stability is indemnified by the shape of the reflexed airfoil with the help of the 3 propellers available. The winglet reimburses the directional stability with the help from the propellers as well.

3.2.5.1 Longitudinal stability

Theoretically, in order for the UAV to achieve longitudinal stability, the moment slope coefficient ($C_{m\alpha}$) must be less than zero (negative) while the zero angle of attack for moment coefficient about the centre of gravity ($C_{m0_{cg}}$) must be greater than zero (Positive). A software tool called XFLR5 is used to analyse the longitudinal stability of the design. XFLR5 is able to generate the graph of moment coefficient against angle

of attack which it can be used to compare with the theoretical graph as shown in Figure 3.4. The comparison will help to determine the longitudinal stability of the UAV.

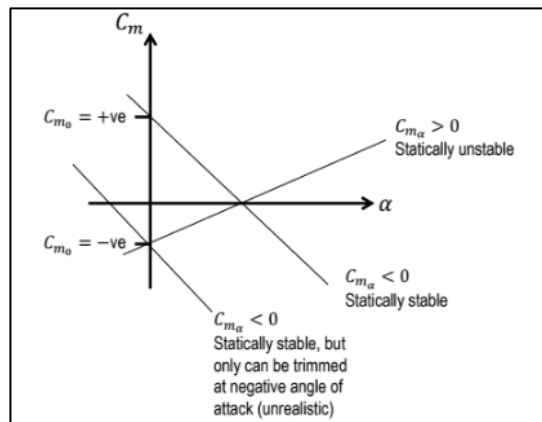


Figure 3.4: Graph of moment coefficient against angle of attack (Nelson, 1998)

3.2.5.2 Lateral Control – Aileron

Lateral stability of the UAV is achieved by using the proper aileron sizing. Ailerons are situated at the outboard of the trailing edge of the wing. The main function of ailerons is to control the rolling of the UAV (Sadraey, 2012b). Thus, the left and right ailerons are deflected differentially and simultaneously to generate the rolling moment about the x-axis. As suggested by Mohammad Sadraey (Sadraey, 2012b), the typical guidance for the ailerons sizing is listed in Table 3.5.

Table 3.5: Typical guidance for the ailerons sizing

No.	Parameter	Value
1	$\frac{S_a}{S_{wing}}$	0.05 – 0.1
2	$\frac{C_a}{c_{wing}}$	0.15 – 0.25
3	$\frac{b_a}{b_{wing}}$	0.2 – 0.3
4	$\frac{b_{ai}}{b_{wing}}$	0.6 – 0.8
5	$\pm\delta_{Amax}$	$\pm 30^\circ$

Note that Figure 3.5 shows the labelling of the symbols for aileron where S_a is the aileron planform area, C_a is aileron chord, b_a is the aileron span and b_{ai} is the location of inner edge of the aileron along the wing span.

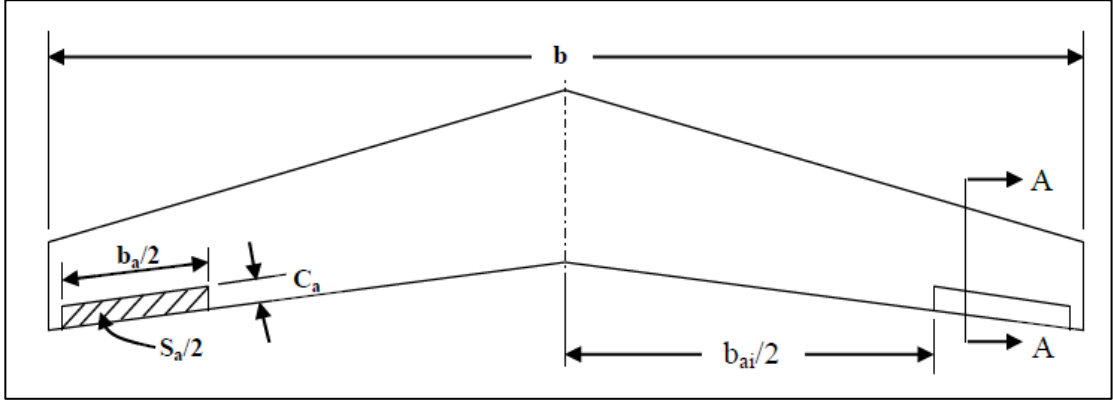


Figure 3.5: Top view wing and aileron (Sadraey, 2012b)

3.2.5.3 Directional control – Winglet

In this project, the design does not have a traditional empennage as this is a tailless concept design. As mentioned in Chapter 2, the winglets attached to the wing tips came with two functions; they are higher aerodynamic performance and directional stability enhancement. Suggested by Jeffrey V.Hogge (V.Hogge, 2008), the winglet sizing is assumed to be a single vertical stabilizer.

Initially, the mean aerodynamic chord for the stabilizer can be calculated by using Equation (18).

$$c_V = \frac{2}{3} C_{V_{root}} \left(\frac{1 + \lambda_V + \lambda_V^2}{1 + \lambda_V} \right) \quad (18)$$

The root tip chord of the stabilizer ($C_{V_{root}}$) follows the dimension of the wing tip chord. The tapered ratio of the stabilizer (λ_V) was set to 0.5 as suggested by Jeffrey V.Hogge (V.Hogge, 2008).